Marked drop in intertidal SST after the arrival of cyclone Dorian to the Atlantic Canadian coast

Ricardo A. Scrosati

St. Francis Xavier University, Marine Ecology Lab, Antigonish, Nova Scotia B2G 2W5, Canada

Email: rscrosat@stfx.ca. Phone: 1-902-867-5289.

Abstract

In intertidal environments, temperature fluctuations at hourly temporal scales are ecologically relevant because of the physiological stress that organisms must endure as a result. Tides constitute the main source of such changes, as low tides periodically expose intertidal habitats to aerial conditions, which can exhibit unusually high and low temperatures in summer and winter, respectively. The present study identifies another source of strong hourly thermal variation, one that acts only upon seawater (not air) temperature. Shortly after the arrival of cyclone Dorian to the Atlantic Canadian coast in September 2019, in-situ loggers revealed that sea surface temperature (SST) decreased in a matter of hours by 10-12 °C in intertidal environments. Data from online environmental services indicated that neither tidal amplitude nor air temperature were likely responsible for this marked SST drop. Conversely, data on wind speed support the notion that shear-induced vertical mixing of the water column caused by this cyclone was the main reason for the pronounced intertidal cooling. This is in line with previous studies that found offshore SST drops with tropical hurricanes. It remains to be seen how the observed decrease in SST may have affected intertidal organisms, as they were acclimated to summer conditions when Dorian hit the coast. As the frequency and intensity of cyclones in temperate latitudes is predicted to increase with climate change, cyclone-related intertidal thermal ecology might deserve further attention.

Keywords: Cyclone · Hurricane · Intertidal · Sea surface temperature · SST

Introduction

In intertidal habitats, temperature can vary considerably at temporal scales of hours. Understanding the causes of such changes is important because abiotic variability can be as ecologically relevant as mean conditions (Bennedetti-Cecchi et al. 2006; Somero 2007). Tides have long been recognized as a central factor influencing intertidal temperature at hourly scales (Helmut et al. 2002; Finke et al. 2007). The reason is that, during low tides, intertidal habitats are exposed to aerial conditions, with temperatures that often differ from seawater temperature. Air temperature during low tides can be extreme under severe weather conditions, such as on hot days in spring and summer (Lathlean et al. 2014; Umanzor et al. 2017) or cold days in winter (Scrosati 2011). Factors such as macroalgal cover (Watt and Scrosati 2013; Scrosati and Ellrich 2018) and a stable cover of ice (Scrosati and Eckersley 2007) can limit thermal extremes during low tides.

Other short-term changes in intertidal temperature are caused by factors that influence only seawater temperature. For example, coastal upwelling can drive deep, cool waters to the surface in a matter of hours (Kämpf and Chapman 2016), in that way cooling intertidal environments during high tides (Tapia et al. 2009). Coastal upwelling is common in many parts of the world and is typically driven by alongshore winds in concert with the Coriolis force (Shan et al. 2016) or by tidal mixing (Chegini et al. 2018). Given its capacity for vertical mixing of upper ocean layers (Seroka et al. 2016; Liu et al. 2018), cyclonic activity might also generate significant thermal fluctuations in intertidal habitats at hourly scales. However, this seems not to have been examined quantitatively, probably because of the low frequency of occurrence of coastal cyclones in comparison with the processes mentioned above. To address this knowledge gap, the present study investigates the marked intertidal cooling that occurred on the Atlantic Canadian coast after the arrival of cyclone Dorian in 2019.

Methods

Dorian approached Canada as a hurricane from southern waters, making landfall on the Canadian coast as a post-tropical cyclone near Halifax, Nova Scotia, at 19:15 on 7 September 2019 (AccuWeather 2019; NOAA 2019). To evaluate Dorian's effects on intertidal temperature on the Nova Scotia coast, this study uses data on sea surface temperature (SST) measured at two intertidal locations separated by 43 km: Deming Island (N 45.2121, W 61.1738) and Barachois

Head (N 45.0890, W 61.6933; Fig. 1). Both locations face the open waters of the Atlantic Ocean directly, without any physical obstructions. The substrate of both locations is stable bedrock. To make Dorian's thermal signal most evident, SST data measured between 1-16 September 2019 are hereby used.

At each location, SST was measured with a submersible logger (HOBO Pendant logger, Onset Computer, Bourne, MA, USA) that was permanently attached to the intertidal substrate by plastic cable ties secured to eye screws drilled into the substrate, allowing almost no contact between the logger and the substrate. The loggers recorded temperature every 30 min. From the two resulting time series, values describing SST were extracted. Such values were the temperature values recorded closest to the time of the successive peaks of high tide, when the loggers were fully submerged in seawater. The time of such tides was determined using information for the tide reference stations that are closest to the studied intertidal locations: Whitehead (N 45.2333, W 61.1833) for Deming Island and Port Bickerton (N 45.1000, W 61.7333) for Barachois Head (Tide and Current Predictor 2019).

To examine how Dorian's winds reached the studied intertidal locations, data on hourly wind speed and daily maximum gusts were retrieved for the weather stations that are closest to the studied intertidal locations: Hart Island (N 45.35, W 60.98) for Deming Island and Beaver Island (N 44.82, W 62.33) for Barachois Head (Government of Canada 2019). To exclude tidal amplitude as a possible explanation for the SST drop measured shortly after Dorian (see Results), the height of the highest tide of each day (proxy for tidal amplitude) was retrieved for Whitehead and Port Bickerton (Tide and Current Predictor 2019), under the notion that coastal SST changes are favoured by spring tides (instead of neap tides) due to increased mixing (Kang and Lee 2014; Shanks et al. 2014; Iwasaki et al. 2015). To exclude air temperature as a potential explanation for the SST drop measured shortly after Dorian (see Results), data on hourly air temperature were retrieved for Hart Island and Beaver Island (Government of Canada 2019).

Results

Before Dorian's landfall on the Canadian coast on 7 September, SST exhibited relatively small changes from day to day, staying between 19-20 °C at Deming Island and 17-21 °C at Barachois Head (Figs. 2-3). After Dorian's arrival, however, SST dropped sharply and quickly at both locations, reaching 9.7 °C at Deming Island and 6.8 °C at Barachois Head at 18:30 on 8

September (Figs. 2-3). By 9 September, SST reached higher levels again, but stayed only around 15 °C at Deming Island and mostly between 12-17 °C at Barachois Head for the remainder of the study (Figs. 2-3).

Coastal surface winds barely surpassed 40 km h^{-1} before 7 September (Figs. 2-3). However, during 7 September, winds intensified dramatically as Dorian's centre reached the shore, reaching hourly values of 88 km h^{-1} near Deming Island and 106 km h^{-1} near Barachois Head (Figs. 2-3), with gusts up to 126 km h^{-1} near Deming Island and 145 km h^{-1} near Barachois Head. After Dorian left the region, and for the remainder of this study, values of wind speed remained similar to those measured before this cyclone (Figs. 2-3).

The passage of Dorian through the studied region during 7-8 September coincided with neap tides, not spring tides (Figs. 2-3). During this study, air temperature often decreased during night hours, increasing again during daytime (Figs. 2-3). Thus, the pronounced drop in SST that occurred mainly during daytime on 8 September largely coincided with an increase in air temperature.

Discussion

The present study has identified a marked drop of SST in intertidal environments on the open Atlantic coast of Nova Scotia shortly after cyclone Dorian made landfall. During the 24 hours after the centre of this cyclone reached the coast, intertidal SST decreased by 10-12 °C. This is a stronger decrease in SST than those caused within one day (up to 6 °C) by upwelling resulting from wind and Coriolis forcing on the Nova Scotia coast in summer (Scrosati and Ellrich 2020). In fact, the SST drop observed after Dorian rivals intertidal thermal drops caused by exposure to the air during low tides in cold winter days, which can decrease intertidal temperature (which remains near 0 °C during high tides) by up to 14 °C when air temperature is low enough on the Nova Scotia coast (Scrosati 2011).

The additional data revealed that neither tidal amplitude nor air temperature were likely responsible for the strong intertidal SST drop recorded on 8 September. On marine shores, the highest tidal amplitudes occur during periods of spring tides. Compared with neap tides, spring tides can favour the cooling of coastal surface waters due to increased vertical mixing (Kang and Lee 2014; Shanks et al. 2014; Iwasaki et al. 2015). However, on the studied coast, SST changes were either small (Barachois Head) or unnoticeable (Deming Island) during spring tides, suggesting a negligible influence, if any, of neap tides on SST. As the marked SST drop of 8 September occurred during neap tides, tidal amplitude then seems to have played little-to-no influence, a conclusion that was also reached for offshore SST decreases in relation to hurricane activity (Miles et al. 2017). Regarding air temperature, the marked intertidal SST drop of 8 September occurred mostly during daytime, and the main cooling period actually coincided with an increase in air temperature. In fact, similar daytime increases in air temperature were common during the study period. Thus, air temperature seems not to have played a role in the pronounced decrease of intertidal SST after Dorian either.

The wind data strongly indicate that cyclone Dorian was, in fact, the cause of the marked decrease of intertidal SST on 8 September. At lower latitudes, tropical hurricanes decrease SST in offshore environments due to shear-induced vertical mixing of waters, as subsurface layers of the ocean are typically cooler than surface layers, especially in summer (Korobkin et al. 2009; Lai et al. 2015; Seroka et al. 2016; Liu et al. 2018). The relative stability of intertidal SST on the Nova Scotia coast for days before Dorian's arrival suggests that coastal waters were then stratified to an extent, Dorian causing intertidal cooling through vertical mixing. The timing of the observed cooling after the passage of Dorian agrees with observations made for tropical hurricanes (Rao et al. 2004). Interestingly, by 9 September, intertidal SST increased again and regained pre-Dorian levels of temporal stability, but staying on average 4-5 °C lower than before Dorian. This pattern is in line with an inertial mixing period after direct cyclone forcing (Rao et al. 2004).

The consequence of such a sharp drop in SST on the physiology of intertidal organisms is unknown, but it may not be small given that the cyclone occurred in summer, when organisms are acclimated to warm air and water temperatures. As cyclone activity is expected to grow in intensity with climate change in temperate latitudes (Knutson et al. 2013; Kossin et al. 2014), cyclone-related intertidal thermal ecology might deserve further attention.

Acknowledgements

This study was funded by a Discovery Grant from the Natural Sciences and Engineering Research Council (NSERC) and by a Leaders Opportunity Grant from the Canada Foundation for Innovation (CFI) awarded to the author. Thanks are also extended to Julius A. Ellrich for his assistance with the maintenance and operation of the loggers.

References

AccuWeather. 2019. Dorian made 6th landfall at Nova Scotia; thousands without power. https://www.accuweather.com/en/weather-news/dorain-made-5th-landfall-as-it-reaches-nova-scotia/70009277

Bennedetti-Cecchi, L., I. Bertocci, S. Vaselli, and E. Maggi. 2006. Temporal variance reverses the impact of high mean intensity of stress in climate change experiments. Ecology 87: 2489–2499.

Chegini, F., Y. Lu, A. Katavouta, and H. Ritchie. 2018. Coastal upwelling off southwest Nova Scotia simulated with a high-resolution baroclinic ocean model. Journal of Geophysical Research: Oceans 123: 2318–2331.

Finke, G.R., S.A. Navarrete, and F. Bozinovic. 2007. Tidal regimes of temperate coasts and their influences on aerial exposure for intertidal organisms. Marine Ecology Progress Series 343: 57–62.

Government of Canada. 2019. Past weather and climate. Historical data. http://climate.weather.gc.ca/historical_data/search_historic_data_e.html

Helmuth, H., C.D.G. Harley, P.M. Halpin, M. O'Donnell, G.E. Hofmann, and C.A. Blanchette. 2002. Climate change and latitudinal patterns of intertidal thermal stress. Science 298: 1015–1017.

Iwasaki, S., A. Isobe, and Y. Miyao. 2015. Fortnightly atmospheric tides forced by spring and neap tides in coastal waters. Scientific Reports 5: article 10167.

Kämpf, J., and P. Chapman. 2016. Upwelling systems of the world. A scientific journey to the most productive marine ecosystems. Cham: Springer.

Kang, K.R., and S.R. Lee. 2014. Variation of the summer low SST area in the southwestern coast of Korea. Geosciences Journal 18: 231–239.

Knutson, T.R., J.J. Sirutis, G.A. Vecchi, S. Garner, M. Zhao, H.S. Kim, M. Bender, R.E. Tuleya, I.M. Held, and G. Villarini. 2013. Dynamical downscaling projections of twenty-first-century Atlantic hurricane activity: CMIP3 and CMIP5 model-based scenarios. Journal of Climate 26: 6591–6617.

Korobkin, M., E. D'Sa, and D.S. Ko. 2009. Satellite observations and NCOM assessment of the Mississippi-Louisiana-Texas coast following hurricanes Gustav and Ike. Naval Research Laboratory, Stennis Space Center, MS, USA, Report No. NRL/PP/7320-09-9322.

Kossin, J.P., K.A. Emanuel, and G.A. Vecchi. 2014. The poleward migration of the location of tropical cyclone maximum intensity. Nature 509: 349–352.

Lathlean, J.A., D.J. Ayre, and T.E. Minchinton. 2014. Estimating latitudinal variability in extreme heat stress on rocky intertidal shores. Journal of Biogeography 41: 1478–1491.

Lai, Q.Z., L.G. Wu, and C.L. Shie. 2015. Sea surface temperature response to typhoon Morakot (2009) and its influence. Journal of Tropical Meteorology 21: 111–120.

Liu, Y., R.H. Weisberg, J. Law, and B. Huang. 2018. Evaluation of satellite-derived SST products in identifying the rapid temperature drop on the West Florida Shelf associated with hurricane Irma. Marine Technology Society Journal 52: 43–50.

Miles, T., G. Seroka, and S. Glenn. 2017. Coastal ocean circulation during hurricane Sandy. Journal of Geophysical Research: Oceans 122: 7095–7114.

NOAA. 2019. National Oceanic and Atmospheric Administration. Historical hurricane tracks. https://coast.noaa.gov/hurricanes

Rao, A.D., S.V. Babu, and S.K. Dube. 2004. Impact of a tropical cyclone on coastal upwelling processes. Natural Hazards 31: 415–435.

Scrosati, R.A. 2011. Subarctic shores without an ice foot: low extremes in intertidal temperature during winter. Current Development in Oceanography 3: 153–160.

Scrosati, R., and L.K. Eckersley. 2007. Thermal insulation of the intertidal zone by the ice foot. Journal of Sea Research 58: 331–334.

Scrosati, R.A., and J.A. Ellrich. 2018. Thermal moderation of the intertidal zone by seaweed canopies in winter. Marine Biology 165: article 115.

Scrosati, R.A., and J.A. Ellrich. 2020. Marked contrast in wind-driven upwelling on the southeastern Nova Scotia coast in July of two years differing in ENSO conditions. Oceanological and Hydrobiological Studies 49, in press.

Seroka, G., T. Miles, Y. Xu, J. Kohut, O. Schofield, and S. Glenn. 2016. Hurricane Irene sensitivity to stratified coastal ocean cooling. Monthly Weather Review 144: 3507–3530.

Shan, S., J. Sheng, K. Ohashi, and M. Dever. 2016. Assessing the performance of a multi-nested ocean circulation model using satellite remote sensing and in-situ observations. Satellite Oceanography and Meteorology 1: 39–59.

Shanks, A.L., S.G. Morgan, J. MacMahan, A.J.H.M. Reniers, M. Jarvis, J. Brown, A. Fujimura, and C. Griesemer. 2014. Onshore transport of plankton by internal tides and upwelling-relaxation events. Marine Ecology Progress Series 502: 39–51.

Somero, G. 2007. Heat stress. In Encyclopedia of tidepools and rocky shores, ed. M.W. Denny, and S.D. Gaines, 266–270. Berkeley: University of California Press.

Tapia, F.J., S.A. Navarrete, M. Castillo, B.A. Menge, J.C. Castilla, J. Largier, E.A. Wieters, B.L. Broitman, and J.A. Barth. 2009. Thermal indices of upwelling effects on inner-shelf habitats. Progress in Oceanography 83: 278–287.

Tide and Current Predictor. 2019. Tidal height and current site selection. http://tbone.biol.sc.edu/tide/index.html

Umanzor, S., L. Ladah, L.E. Calderón-Aguilera, and J.A. Zertuche-González. 2017. Intertidal macroalgae influence macroinvertebrate distribution across stress scenarios. Marine Ecology Progress Series 584: 67–77.

Watt, C.A., and R.A. Scrosati. 2013. Bioengineer effects on understory species richness, diversity, and composition change along an environmental stress gradient: experimental and mensurative evidence. Estuarine, Coastal and Shelf Science 123: 10–18.

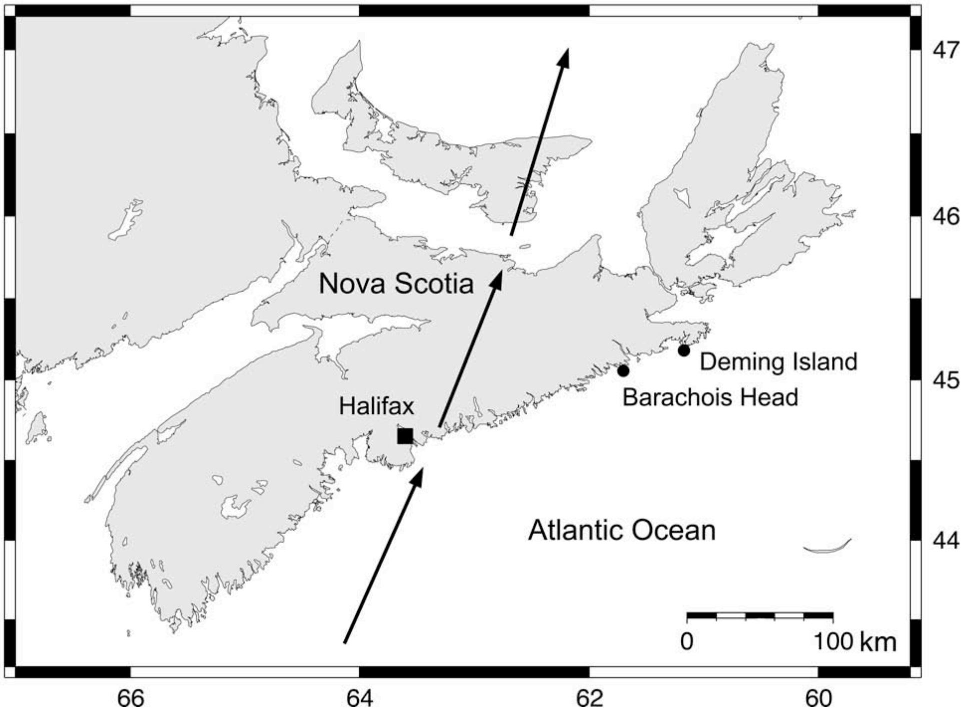

Fig. 1. Map of Nova Scotia, showing the position of the two studied intertidal locations (Deming Island and Barachois Head) and the path of cyclone Dorian's centre (arrows).

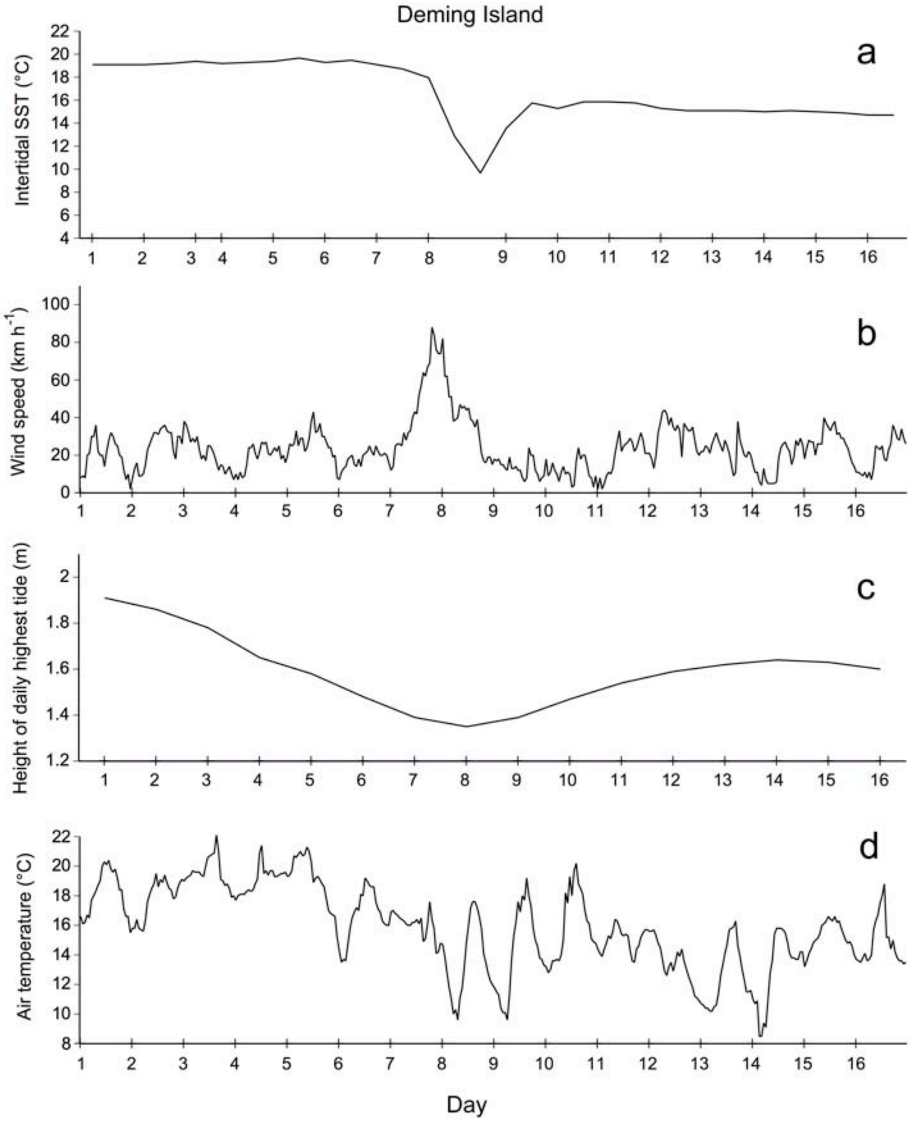

Fig. 2. Environmental trends for Deming Island between 1-16 September 2019: (a) intertidal sea surface temperature (SST), (b) wind speed, (c) height of the daily highest tide (proxy for tidal amplitude), and (d) air temperature. SST data for 8 September include the lowest SST value found for that day, which was recorded 2 h after the second high tide.

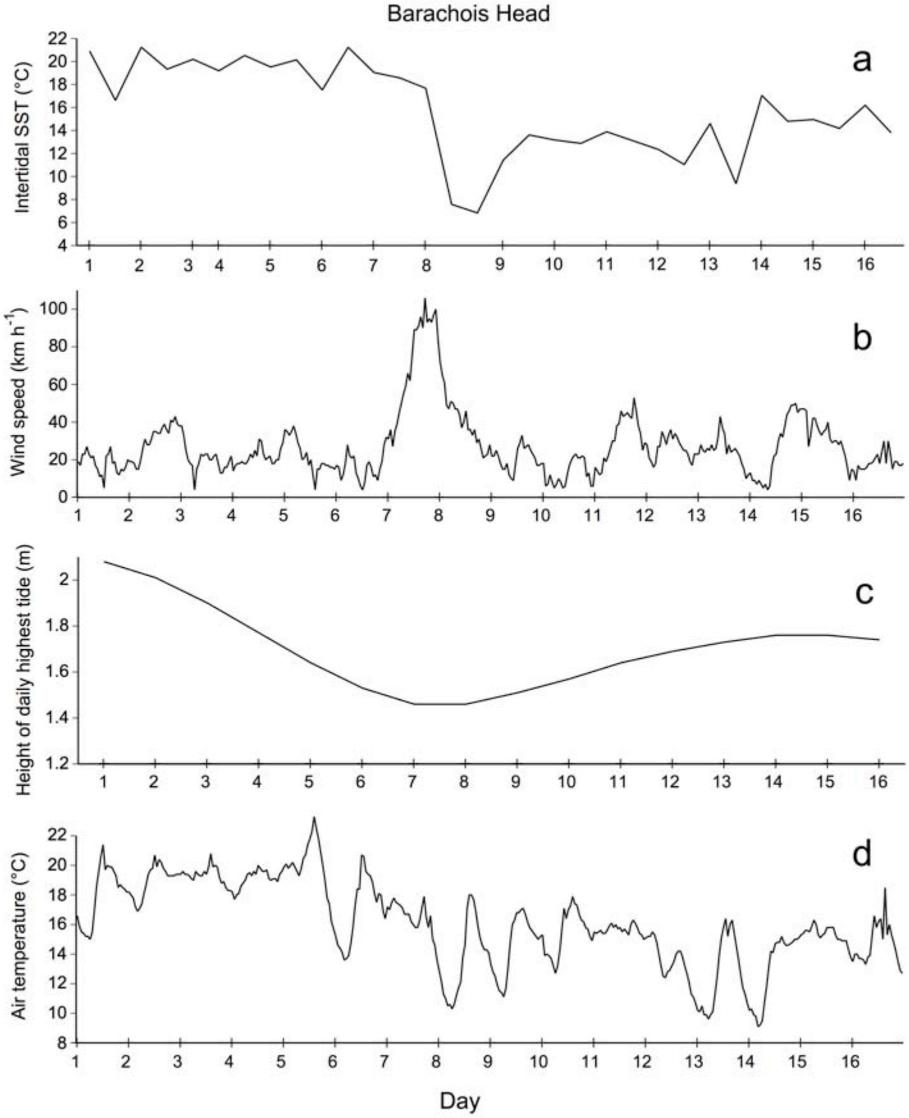

Fig. 3. Environmental trends for Barachois Head between 1-16 September 2019: (a) intertidal sea surface temperature (SST), (b) wind speed, (c) height of the daily highest tide (proxy for tidal amplitude), and (d) air temperature. SST data for 8 September include the lowest SST value found for that day, which was recorded 2 h after the second high tide.